Simultaneous Characterization of Glyco- and Phosphoproteomes of Mouse Brain Membrane Proteome with Electrostatic Repulsion Hydrophilic Interaction Chromatography*[S]

Huoming Zhang‡, Tiannan Guo‡, Xin Li‡, Arnab Datta‡, Jung Eun Park‡, Jie Yang‡, Sai Kiang Lim§, James P. Tam‡, and Siu Kwan Sze‡¶

Characterization of glyco- and phosphoproteins as well as their modification sites poses many challenges, the greatest being loss of their signals during mass spectrometric detection due to substoichiometric amounts and the ion suppression effect caused by peptides of high abundance. We report here an optimized protocol using electrostatic repulsion hydrophilic interaction chromatography for the simultaneous enrichment of glyco- and phosphopeptides from mouse brain membrane protein digest. With this protocol, we successfully identified 544 unique glycoproteins and 922 glycosylation sites, which were significantly higher than those from the commonly used hydrazide chemistry method (192 glycoproteins and 345 glycosylation sites). Moreover, a total of 383 phosphoproteins and 915 phosphorylation sites were recovered from the sample, suggesting that this protocol has the potential to enrich both glycopeptides and phosphopeptides simultaneously. Of the total 995 glycosylation sites identified from both methods, 96% were considered new as they were either annotated as putative or not documented in the newly released Swiss-Prot database. Thus, this study could be of significant value in complementing the current glycoprotein database and provides a unique opportunity to study the complex interaction of two different post-translational modifications in health and disease without being affected by interexperimental variations. ***Molecular & Cellular Proteomics 9:635–647, 2010.***

Protein glycosylation and phosphorylation are two important post-translational modifications. In mammals, it has been estimated that nearly 50% of all proteins are glycosylated (1), and at least one-third of all proteins are phosphorylated (2). The modification of a protein has an important role in determining its stability, activity, localization, and interactions with other proteins. For example, *N*-linked glycosylation of a protein enhances its stability and targets it mainly to extracellular locations such as the plasma membrane (3), whereas phosphorylation of tyrosine kinases initiates signal cascades in both proproliferative and antiapoptotic cellular responses (4).

Membrane proteins are essential for cells to maintain the integrity of their structure and perform signal transduction in response to extracellular stimulation. For most membrane proteins, receptor activities of their extracellular domains are often mediated via *N*-linked glycosylation, whereas the cytoplasmic domains can be phosphorylated reversibly and function as signal transducers. Alteration of these modifications correlates with cellular differentiation, implantation, and tissue development (5, 6). Such alteration is required for the induction of many forms of synaptic plasticity such as long term potentiation and depression in learning and memory formation. For example, aberrant glycosylation and abnormal phosphorylation have been found to be associated with many neurological disorders such as Alzheimer disease (7–9), Parkinson disease (10, 11), Guillain-Barré and Miller-Fisher syndromes (12), and even muscle-eye-brain disease (13). Understanding the brain glyco- and phosphoproteomes is therefore not only essential for studying the biology of these diseases but also aiding drug discovery and translational research as many of the glycoproteins have the potential to be viable drug targets due to the ease of their accessibility on the cell surface.

Study of the glyco- and phosphoproteomes of cell membrane presents a number of challenges mainly due to their low abundance, their large dynamic range, and the inherent hydrophobicity of membrane proteins. It has been estimated that less than 5% of the peptides in a typical complex protein digest are either *N*-linked glycosylated (14) or phosphorylated (15). Therefore, development of efficient protocols for the enrichment of glycopeptides and phosphopeptides is essential for their subsequent detection and identification.

Methods used for the enrichment of glycopeptides and glycoproteins have varied with time and among investigators. Lectin-based affinity enrichment is one of the earliest and most widely used approaches for the analysis of glycoproteins and their associated carbohydrates (16–19). Generally, lectins are highly specific for a particular type of carbohydrate

From the ‡School of Biological Sciences, Nanyang Technological University, 60 Nanyang Drive, Singapore 637551 and §Institute of Medical Biology, 8A Biomedical Grove, 05-505 Immunos, Singapore 138648, Singapore

Received, July 8, 2009, and in revised form, December 30, 2009
Published, MCP Papers in Press, January 4, 2010, DOI 10.1074/mcp.M900314-MCP200

moiety, such as wheat germ lectin, which mainly recognizes GlcNAc, and concanavalin A lectin specific for mannose (20). Combining the use of two or more types of lectins with potentially complementary binding properties is often required to recover a significant number of glycoproteins from a complex sample (18, 21, 22). Another commonly used method is utilizing hydrophilic affinity physicochemical chromatography. This method is based on hydrogen bonding between the hydroxyl group of carbohydrate moieties in glycopeptides and hydrophilic materials such as Sepharose or cellulose (23, 24). Thus, this enrichment has a much wider range in terms of the types of glycoproteins recovered as compared with the lectin-based method. In addition, Ding *et al.* (25) demonstrated that tryptic glycopeptides can be eluted as a set after the tryptic non-glycopeptides in the pure hydrophilic interaction liquid chromatography mode by increasing the hydrophobicity of peptides with trifluoroacetate as an ion-pairing agent. Recently, a method utilizing hydrazide chemistry has gained increasing popularity for the study of the *N*-linked glycoproteome (26, 27). It has been applied to high throughput global analysis of *N*-glycoproteins from various samples such as human serum (28), saliva (29), platelet (30), liver (31), and cancer tissue (32). Although this approach is theoretically able to capture all types of glycoproteins or glycopeptides, a total of only 1522 unique glycosylation sites was collectively identified in nearly 10 studies, representing about 3% of the total predicted glycosylation sites in the human proteome (14). In recent attempts to identify more glycoproteins in a sample and expand coverage of the *N*-linked glycoproteins, different groups have used different methods in parallel to simultaneously analyze a sample. Cao *et al.* (33) utilized the hydrazide method and hydrophilic affinity to identify glycosylation sites in secreted proteins and reported a total of 300 glycosylation sites with 159 and 261 from each of the methods, respectively. Lee *et al.* (22) used the hydrazide method and three lectins for a study of rat liver glycoproteins. They identified a total of 335 glycoproteins with 202 from the lectin method and 210 from the hydrazide method. These studies demonstrated that current methods are complementary; hence, combined use of them could enhance glycoprotein recovery, although the overall efficiency remains relatively low.

As with the need to develop protocols for glycopeptide enrichment, many methods for phosphopeptide enrichment have also been described. These include phosphoramidate chemistry (34), immunoprecipitation with phosphospecific antibodies (35), IMAC (36), strong cation exchange (SCX)[1] chromatography (37), and titanium dioxide (TiO_2) chromatography (38). Each method has its unique advantages and shortcomings and analyzing a sample either by using different methods in parallel or combining different methods into one would often enrich more phosphopeptides and therefore identify more phosphoproteins. Indeed, Villén *et al.* (39) were able to identify more than 5,600 non-redundant phosphorylation sites on 2,300 proteins from mouse liver when using SCX chromatography followed by IMAC affinity purification. Similarly, when coupling SCX with TiO_2 chromatography, Olsen *et al.* (40) reported a total of 6,600 phosphorylation sites on 2,200 HeLa cell proteins. In addition, the TiO_2 and the IMAC method were found to be complementary (41), and using both methods in parallel to analyze a sample generated a combined set of information that surpassed the outcome derived using one method. However, an effective method for simultaneous enrichment of both glyco- and phosphopeptides is highly desirable.

Recently, a novel mode of chromatography termed electrostatic repulsion hydrophilic interaction chromatography (ERLIC) has been introduced for enrichment of phosphopeptides based on both their electrostatic and hydrophilic properties (42). With the low pH and high organic content of the mobile phase, the majority of peptides with carboxyl groups at aspartic acid and glutamic acid residues and the C terminus are largely un-ionized and thus poorly retained by the weak anion exchange (WAX) column, whereas phosphopeptides and highly hydrophilic peptides will interact strongly with the column and are retained. A salt and aqueous gradient can then be used to gradually elute phosphopeptides from the column. Typically, buffer A (10 mM sodium methyl phosphonate and 70% acetonitrile, pH 2.0) and buffer B (200 mM triethylamine phosphate with 60% acetonitrile, pH 2.0) are used to create a gradient for the enrichment and fractionation of the phosphopeptides from a cell lysate digest (43). This enrichment method has been found to be comparable with the hydrazide method in the identification of glycoproteins when a platelet digest was used as a starting material (44). The ERLIC enrichment is mainly based on the negatively charged sialyl group in glycopeptides (44). However, it might be able to enrich other hydrophilic glycopeptides when an oligosaccharide side chain is a large and hydrophilic domain that causes a significant increase in retention time of the peptide in any hydrophilic interaction liquid chromatography-based mode of ERLIC.

We report here an improved protocol using ERLIC for the simultaneous enrichment of glyco- and phosphopeptides from mouse brain membrane preparation. With this protocol, the yields of glycoproteins (544) and glycosylation sites (922) were significantly higher than those from the hydrazide chemistry method (192 glycoproteins and 345 glycosylation sites). In total, 995 glycosylation sites were identified, 96% of which were considered new as they were either annotated as putative or not documented in the newly released Swiss-Prot database. Moreover, a total of 383 phosphoproteins including 915 phosphorylation sites was recovered from the ERLIC

[1] The abbreviations used are: SCX, strong cation exchange; ERLIC, electrostatic repulsion hydrophilic interaction chromatography; LTQ, linear quadrupole ion trap; NCAM, neural cell adhesion molecule; TiO_2, titanium dioxide; WAX, weak anion exchange; IPI, International Protein Index; GO, gene ontology; MGI, Mouse Genome Informatics; KEGG, Kyoto Encyclopedia of Genes and Genomes; APP, amyloid β precursor protein.

approach, suggesting that this protocol has potential for the simultaneous study of both glyco- and phosphoproteomes.

MATERIALS AND METHODS

Mice and Tissue Preparation—All animal procedures were performed according to the protocols approved by Nanyang Technological University for Biological Studies and Animal Care and Use Committees. A single C57BL/6J inbred strain mouse purchased from Centre for Animal Care, National University of Singapore was used in this study. At the age of 8 weeks, the mouse was euthanized with excess isoflurane anesthesia. The whole intact brain was collected, snap frozen in liquid nitrogen, and then stored at −80 °C.

Membrane Protein Extraction and Digestion—Three frozen brains (~1.5 g, wet weight) were ground in liquid nitrogen in a prechilled mortar with pestle. The fine powder was transferred to a 2-ml Eppendorf tube and HES buffer (20 mM HEPES, pH 7.4, 1 mM EDTA, 250 mM sucrose) supplemented with protease inhibitor (10 μl/mg of tissue) (Roche Diagnostics). The sample was sonicated three times on ice using a Vibra Cell™ high intensity ultrasonic processor (Jencon, Leighton Buzzard, Bedfordshire, UK). The remaining debris and unbroken cells were removed by centrifugation at 1000 × *g* at 4 °C for 10 min. The supernatant was transferred to a new tube and centrifuged at 100,000 × *g* at 4 °C for 45 min. The pellet containing membrane fractions was washed once with Na_2CO_3 (0.1 M, pH 11) and twice with Milli-Q water, respectively, followed by centrifugation at 100,000 × *g* at 4 °C. The membrane pellet was then dissolved in 8 M urea solution, and protein content was determined with a 2-D Quant kit (GE Healthcare) according to the manufacturer's instructions. Approximately 6 mg of protein was aliquoted into six tubes and used for subsequent experiments. The proteins were reduced with 10 mM tris(carboxyethylphosphine) hydrochloride for 30 min at 37 °C and alkylated with 40 mM iodoacetamide for 1 h at room temperature. Proteins were then diluted 7-fold with 50 mM NH_4HCO_3 prior to digestion with trypsin (Promega, Madison, WI) overnight at 37 °C in a 1:50 trypsin-to-protein mass ratio. The protein digests were desalted using Sep-Pak C_{18} cartridges (Waters) and dried in a SpeedVac (Thermo Electron, Waltham, MA).

Enrichment of N-Linked Glycopeptides and Phosphopeptides Using ERLIC—ERLIC buffer A (10 mM sodium methyl phosphonate with 70% acetonitrile, pH 2.0) was prepared by addition of NaOH to a solution of methylphosphonic acid (Sigma-Aldrich) in water followed by addition of acetonitrile. Buffer B (200 mM triethylamine phosphate with 25% acetonitrile, pH 2.0) was prepared by addition of triethylamine (Sigma-Aldrich) to a solution of phosphoric acid in water followed by addition of acetonitrile. A total of 3 mg of protein digest was used for three replicate ERLIC runs. For each run, ~1 mg of digest reconstituted in 200 μl of buffer A was loaded into a PolyWAX LP™ column (4.6 × 200 mm, 5-μm particle size, 300-Å pore size; PolyLC, Columbia, MD) on a Prominence™ HPLC unit (Shimadzu, Kyoto, Japan). The sample was fractionated using a gradient of 100% buffer A for 10 min, 0–30% buffer B for 25 min, 30–100% buffer B for 5 min, and finally 100% buffer B for 10 min at a constant flow rate of 1 ml/min for a total of 50 min. The eluted fractions were monitored via a UV detector at 214 nm wavelength. Fractions were collected at 1-min intervals and dried in a SpeedVac. The consecutive fractions were combined, and finally a total of seven fractions was obtained prior to desalting using Sep-Pak C_{18} solid phase extraction cartridges (Waters). The samples were then dried, reconstituted into 30 μl of 50 mM NH_4HCO_3, and treated with 500 units/μl peptide-*N*-glycosidase F (New England Biolabs, Ipswich, MA) at 37 °C overnight. All samples were acidified with addition of 1.5 μl of 100% formic acid and dried in a SpeedVac.

Enrichment of N-Linked Glycopeptides Using Hydrazide Chemistry—As with the ERLIC enrichment, a total of 3 mg of protein digest was used for experiments in triplicate with each using 1 mg of digest. The glycopeptides were enriched using the published protocols (26, 27) with some modifications. Briefly, the dried protein digests were dissolved in 200 μl of coupling buffer (100 mM sodium acetate, 150 mM sodium chloride, pH 5.5) and oxidized by incubation with sodium periodate (final concentration of 10 mM) in the dark for 30 min at room temperature. The reaction was stopped by incubating with a final concentration of 20 mM sodium sulfite solution for 10 min. The oxidized peptides were then coupled with 50 μl of prewashed Affi-Gel hydrazide gel (Bio-Rad) overnight at room temperature with end-over-end rotation. After the coupling, the gel was washed twice sequentially with 1 ml of H_2O, 1.5 M sodium chloride, methanol, acetonitrile, and 50 mM NH_4HCO_3 to remove nonspecific binding. The glycopeptides were then enzymatically released from the gel by incubation with 200 μl of peptide-*N*-glycosidase F in 50 mM NH_4HCO_3 (500 units/μl) at 37 °C overnight. After centrifugation at 500 × *g*, the supernatant was collected, and the gel was washed with 200 μl of 50 mM NH_4HCO_3, 50% acetonitrile, and 80% acetonitrile sequentially. The supernatant and all washings were combined, acidified with formic acid, and dried in a SpeedVac.

Mass Spectrometric Analysis—Each dried fraction was reconstituted in 100 μl of 0.1% formic acid and analyzed twice using an LTQ-FT Ultra mass spectrometer (Thermo Electron) coupled with a Prominence™ HPLC unit (Shimadzu). For each analysis, 50 μl of the samples was injected from an autosampler (Shimadzu) and concentrated in a Zorbax peptide trap (Agilent, Palo Alto, CA). The peptide separation was performed in a capillary column (200-μm inner diameter × 10 cm) packed with C_{18} AQ (5-μm particles, 300-Å pore size; Michrom Bioresources, Auburn, CA). Mobile phase A (0.1% formic acid in H_2O) and mobile phase B (0.1% formic acid in acetonitrile) were used to establish the 90-min gradient comprising 3 min of 0–5% B and then 52 min of 5–25% B followed by 19 min of 25–80% B, maintenance at 80% B for 8 min, and finally re-equilibration at 5% B for 8 min. The HPLC system was operated at a constant flow rate of 30 μl/min, and a splitter was used to create a flow rate of ~500 nl/min at the electrospray emitter (Michrom Bioresources). The sample was injected into an LTQ-FT through an ADVANCE™ CaptiveSpray™ source (Michrom Bioresources) with an electrospray potential of 1.5 kV. The gas flow was set at 2, ion transfer tube temperature was 180 °C, and collision gas pressure was 0.85 millitorr. The LTQ-FT was set to perform data acquisition in the positive ion mode as described previously (43). Briefly, a full MS scan (350–2000 *m/z* range) was acquired in the FT-ICR cell at a resolution of 100,000 and a maximum ion accumulation time of 1000 ms. The automatic gain control target for FT was set at 1e+06, and precursor ion charge state screening was activated. The linear ion trap was used to collect peptides and to measure peptide fragments generated by CID. The default automatic gain control setting was used (full MS target at 3.0e+04, MS^n at 1e+04) in the linear ion trap. The 10 most intense ions above a 500-count threshold were selected for fragmentation in CID (MS^2), which was performed concurrently with a maximum ion accumulation time of 200 ms. An MS^3 scan was followed after each MS^2 scan when neutral losses of 98 Da for 1+, 49 Da for 2+, or 32.7 Da for 3+ ions were detected. Dynamic exclusion was activated for this process with a repeat count of 1, exclusion duration of 20 s, and ±5-ppm mass tolerance. For CID, the activation Q was set at 0.25, isolation width (*m/z*) was 2.0, activation time was 30 ms, and normalized collision energy was 35%.

Database Searching—All MS and MS/MS data were searched using both Sequest in Bioworks Browser (version 3.3, Thermo Fisher Scientific Inc.) and Mascot (version 2.2.04, Matrix Science, Boston, MA) search engines. The IPI mouse protein database (45) (version 3.55; 55,956 sequences) and its reversed complement were combined and used for the searches. For the Sequest search, the peak

TABLE I
Summary of experiment statistics

	Peptides/ experiment	Replicates	No. of fractions	No. of MS injections	Sample preparation time	MS time	Database searches
	mg				*days*	*h*	
ERLIC	1	3	21	42	~1	63	Mascot, Sequest
Hydrazide method	1	3	3	6	~2	9	Mascot, Sequest

lists (dta files) were first generated from the raw data by Bioworks Browser (version 3.3, Thermo Fisher Scientific Inc.) for the search. For the Mascot search, the raw data were first converted into the dta format using the extract_msn (version 4.0) in the Bioworks Browser. These dta files were then converted into Mascot generic file format using an in-house program prior to the Mascot search as described (46). In both searches, enzyme limits were set at full tryptic cleavage at both ends; a maximum of two missed cleavages was allowed; mass tolerances of 10 ppm for peptide precursors was used; carboxamidomethylation (+57.02) at cysteine residues was set as a fixed modification; and oxidation (+15.99) at methionine, phosphorylation at serine, threonine, or tyrosine (+79.96), and deamidation (+0.98) at asparagine or glutamine were set as variable modifications. A mass tolerance of 0.5 Da was set for fragment ions in both Mascot and Sequest searches. To achieve high confidence identification, peptide matches were filtered with an expectation value of less than 0.05 in the Mascot search and peptide probability cutoff of 0.05, $\Delta Cn > 0.08$, and XCorr cutoffs of 1.5, 2.0, and 2.5 for 1+, 2+, and 3+ charged peptides, respectively, in the Sequest search. After filtering, the false positive rates (FPR $= 2 \times N_{rev}/N_{total}$ where N_{rev} is the number of peptides identified from the reversed sequences and N_{total} is the number of total peptides identified) for the ERLICs and the hydrazides were estimated to be 0.82 and 1.3% via Mascot search and 0.75 and 1.7%, respectively, via Sequest by the "target-decoy" database search strategy (47). Peptides identified with a consensus N*X*(S/T) (with *X* not proline) and a modification of deamidation at the Asn were regarded as *N*-linked glycopeptides. The deamidation (Asn to Asp) can be wrongly assigned from database searches if an isotopic peak of a precursor is incorrectly assigned as a "monoisotopic peak." This occurs occasionally when a precursor ion signal is weak. To eliminate such false positive assignments, we integrated the area of the peak located immediately before the assigned monoisotopic peak and filtered out the assignments when the peak area over the monoisotopic peak was above 1%. Furthermore, a set of non-redundant glycoproteins was reported by inclusion of only the protein isoform with a higher protein score assigned by the database search engines when the protein isoforms share the same glycopeptides. The peptide/protein lists obtained were either exported to Microsoft Excel or processed using in-house scripts for further analysis.

Protein Classification and Functional Annotation—Subcellular and functional categories were based on the annotations of gene ontology (GO) using the MGI GO_Slim Chart Tool. Signal peptides were predicted using SignalP 3.0 (48). The number of transmembrane helices of all identified glycoproteins was predicted using TMHMM 2.0 (49). Cell surface, secreted, and transmembrane proteins were classified based on SignalP and TMHMM information and were grouped as extracellular proteins as described (14). Pathway analysis was performed based on the Kyoto Encyclopedia of Genes and Genomes (KEGG) pathway collection (50).

RESULTS AND DISCUSSION

Experimental Design—Recovery of glyco- and phosphoproteins as well as their modification sites poses many challenges, the greatest being the loss of the low abundance glyco- and phosphopeptides during isolation and detection. To maximize the recovery of glyco- and phosphoproteins from the mouse brain membrane preparation, we adopted a unique combination of individually successful approaches such as subfractionation to obtain a purified membrane fraction (51) followed by parallel use of two enrichment approaches with potentially high efficiency (hydrazide chemistry and ERLIC). This was finally coupled to duplicate MS analysis and two types of database searches (Table I) that ensured statistical consistency and better coverage for identification.

The glycopeptide capture based on hydrazide chemistry has been standardized and widely used (26, 27), whereas ERLIC is a relatively new method. Initial adaptations of the ERLIC protocol for phosphopeptide binding and elution to the capture of glycopeptides yielded a number of glycoproteins comparable to that of the hydrazide method (44). As phosphopeptides and glycopeptides differ in their charge and hydrophilicity, we hypothesized that the retention time and optimal elution conditions for glycopeptides would be different from those for phosphopeptides. Indeed, we found that many glycopeptides did not elute until a low organic content (~30%) was reached. The broader gradient window for the elution of glycopeptides (70–30% organic content) as compared with phosphopeptides (70–60%) is probably due to the higher complexity and heterogeneity of carbohydrate moieties. Thus, a new buffer system consisting of buffer A (10 mM sodium methyl phosphonate and 70% acetonitrile, pH 2.0) and buffer B (200 mM triethylamine phosphate with 25% acetonitrile, pH 2.0) was used for subsequent glyco- and phosphopeptide enrichment and fractionation.

Fig. 1 shows the ERLIC chromatograms for the fractionation of the mouse brain membrane digest. As this study focused on the identification of post-translational modifications, the bulk of peptides eluted in the first 7 min was not collected. In each ERLIC run, a total of 41 fractions from 7 to 48 min was collected, but only seven fractions were finally submitted for LC-MS/MS analysis by combining five consecutive fractions with the exception of the last fraction (Fig. 1, *a* and *b*) as we anticipated the peptide complexity to be substantially reduced such that it was below the detection sensitivity of one-dimensional LC-MS/MS.

Identification of N-Linked Glycoproteins and Glycosylation Sites—Protein identification was achieved by using two search engines, Mascot and Sequest, for the interpretation of the MS/MS spectra. The false positive rate of overall peptide

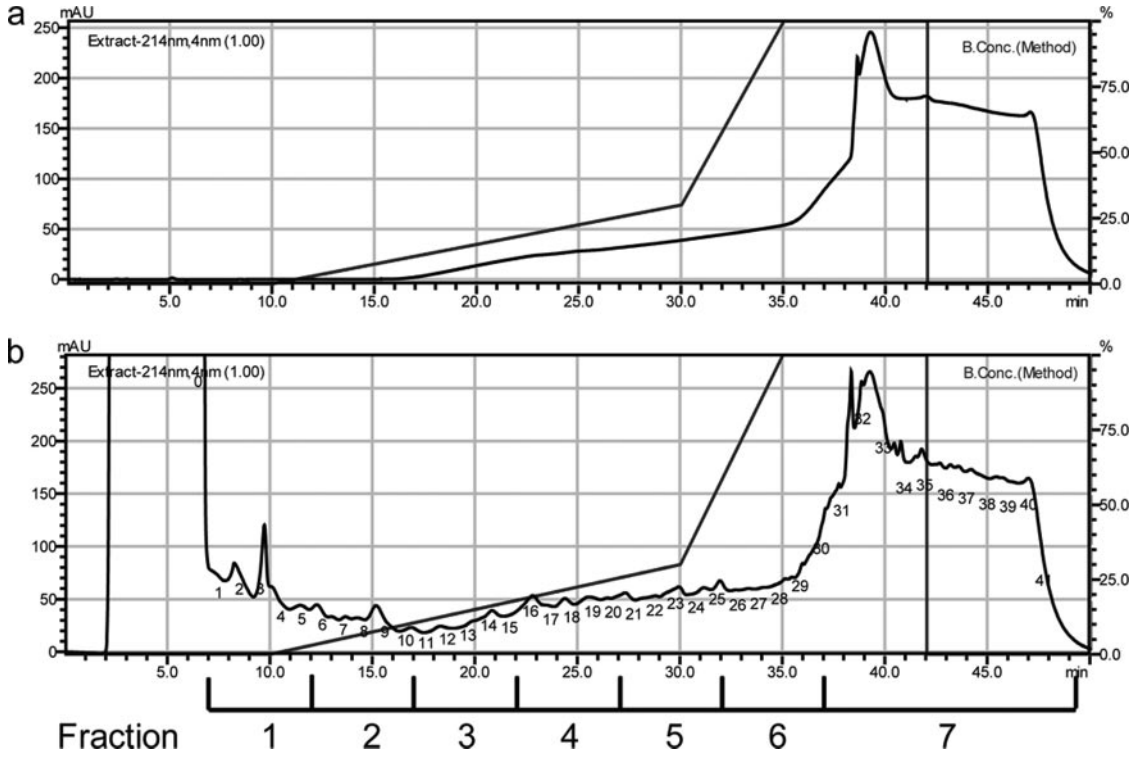

FIG. 1. **ERLIC chromatograms.** *a*, a blank run shows the LC gradient and background UV absorption chromatogram at 214 nm. *b*, 1 mg of mouse brain tryptic digest. Forty fractions from 7 to 50 min were collected and then combined to seven final fractions as shown for LC-MS/MS analysis.

assignment in both searches was controlled within 1%. The numbers of total peptides, glycopeptides, and proteins identified by the two engines were comparable. Identifying the correct isoform of the protein is a common problem of shotgun proteomics studies. This poses a greater challenge in glycoproteomics as a glycopeptide can possibly be assigned to multiple proteins with each having supporting unique peptides. For example, Nrcam isoform 2 and isoform 3 share four glycopeptides but also have respective unique peptides (K ↓ EDAHADPEIQPMKEDDGTFGEYSDAEDHKPLK ↓ K in isoform 2 and K ↓ EKEDAHADPEIQPMKEDDGTFGEYR ↓ S in isoform 3). In this case, we reported only the glycoprotein isoform with a higher protein score assigned by the database search engine to achieve a set of non-redundant glycoproteins. The statistics of identified proteins, peptides, and post-translational modification sites are summarized in supplemental Table 1.

Using the Mascot search engine, a total of 738 unique glycosylation sites assigned to 446 glycoproteins was identified from the three ERLIC replicates (Fig. 2). In contrast, only 259 unique glycosylation sites and 153 glycoproteins were recovered from the three hydrazide replicates. The non-redundant MS/MS spectra of the glycopeptides enriched by the ERLIC and the hydrazide chemistry in Mascot peptide view format are shown in supplemental Data 1 and 4. The numbers of identified glycosylation sites and glycoproteins in the ERLIC approach (mean ± S.D., 560 ± 70 sites; 352 ± 30 glycoproteins) were significantly higher than those from the hydrazide method (216 ± 9 sites; 131 ± 4 glycoproteins) (Fig. 2*c*). In the ERLIC approach, 52.4% of glycosylation sites were common in all three replicates, and an average of 65.5% was found to be overlapping between any two replicates. About 58.3% of the glycoproteins were identified from all three replicates with an average of 70.1% overlapping between any two replicates (Fig. 2*a*). A slightly higher proportion of glycosylation sites (68.3%) and glycoproteins (72.7%) was observed in all three replicates from the hydrazide method (Fig. 2*b*). Clearly, repeated analyses of a single sample enhanced the number of glycosylation sites and glycoproteins identified from the sample as is true of shotgun proteomics in general. Similar results were obtained via a Sequest search: a total of 827 glycosylation sites (528, 704, and 604 from each ERLIC) and 495 glycoproteins (348, 430, and 373, respectively) were identified from the three ERLIC replicates, whereas 283 glycosylation sites (232, 219, and 220 from each hydrazide) and 174 glycoproteins (148, 136, and 140, respectively) were recovered from the three hydrazide replicates. We found that the ERLIC and hydrazide results contained 12.1 and 9.5% non-N*X*(S/T) motif sites, respectively; these sites are likely generated by nonspecific deamidation during the sample preparation.

The advantage of using a combination of search engines is shown in Fig. 3. The use of a second search engine (Sequest) yielded 184 additional glycosylation sites and 98 additional glycoproteins in the ERLICs and an additional 92 sites and 38

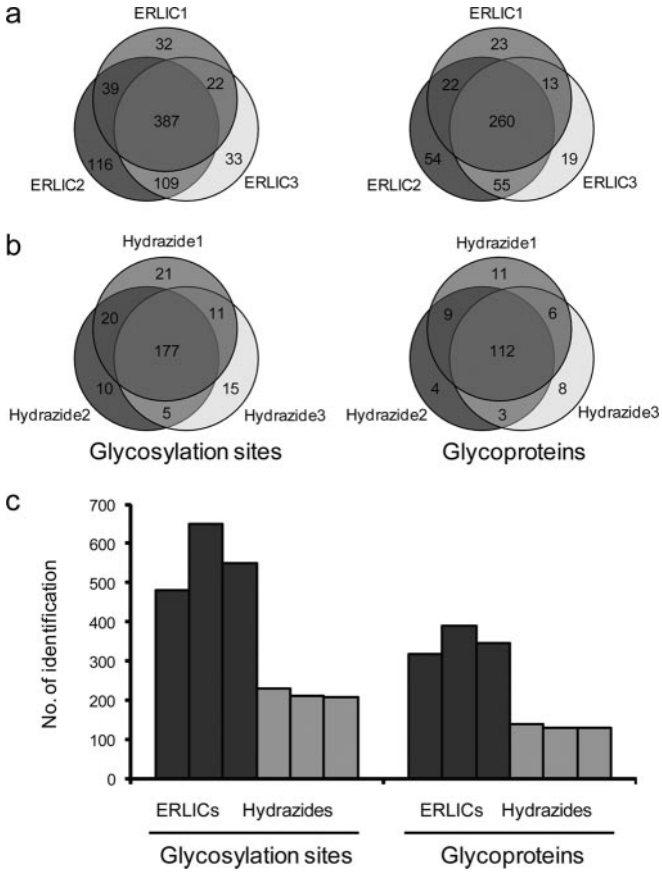

FIG. 2. **Identification of glycosylation sites and glycoproteins using Mascot search engine.** Venn diagrams of glycosylation sites and glycoproteins identified from the ERLICs (*a*) and the hydrazide method (*b*) and a comparison of the number of glycosylation sites and glycoproteins identified from the ERLIC and the hydrazide method (*c*) are shown.

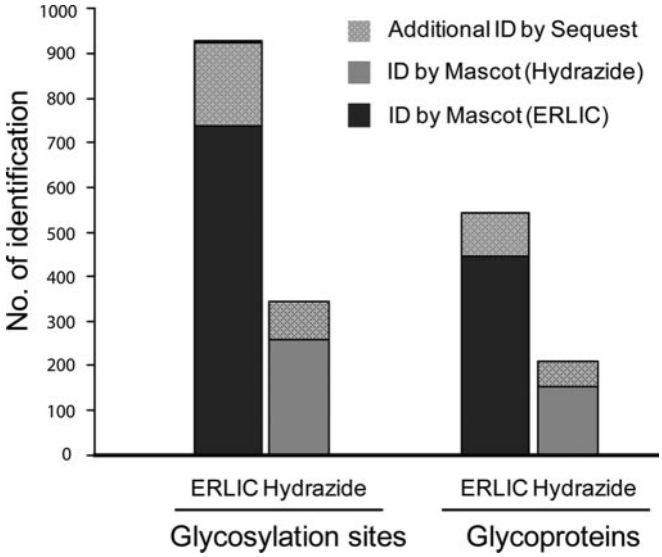

FIG. 3. **Glycosylation sites and glycoproteins identified using two search engines.** Combined use of Mascot and Sequest identified (*ID*) a number of additional sites and proteins.

proteins in the hydrazide run, respectively. Fig. 4 shows the representative spectra that were confidently assigned by one search engine but not the other. Aminopeptidase N (CD13), present in various brain structures (52), was identified with three unique glycopeptides with good Mascot scores of 61, 54, and 50, respectively. In Sequest, the corresponding scores for the three peptides were XCorr 3.29 (R ↓ gNATLVNEADKLR ↓ S, 2+, p 4.8e−8, ΔCn 0.029 where gN is deamidated Asn), XCorr 3.969 (R ↓ FTCgNQTTDVIIIHSK ↓ K, 3+, p 1.0e−9, ΔCn 0.030), and XCorr 4.882 (K ↓ SGQEDHYWLDVEKgNQSAK ↓ F, 3+, p 1.77e−06, ΔCn 0.011), respectively. Although the three peptides have relatively high Sequest scores, all ΔCn values below the set threshold of 0.08 resulted in the failure to identify this protein. On the other hand, CD63, abundantly expressed in neural tissue, was identified from Sequest with two significant peptides but not from Mascot because the scores of both peptides fell below the identity score. The confident identification of a peptide by only one search engine probably reflects the different scoring and probability calculations used by the engines, which are highly dependent on the charge state, residue composition and peptide length, and signal-to-noise ratios of MS/MS spectra (53).

In total, 995 glycosylation sites assigned to 562 non-redundant glycoproteins were identified in this study (Fig. 5). Information for each identified glycoprotein including protein accession number (IPI), protein description, identified glycopeptides, and unique glycosylation sites is listed in supplemental Table 2. Of these, the hydrazide chemistry followed by one-dimensional LC-MS/MS yielded 345 glycosylation sites and 192 glycoproteins, which is comparable to other studies. Lee *et al.* (22) reported 210 glycoproteins from rat liver membrane preparation. Zhang *et al.* (32) identified 445 glycosylation sites from prostate cancer tissue. Enrichment of glycopeptides from more starting material followed by analysis using two-dimensional LC-MS/MS could yield more glycoproteins and glycosylation sites. With this approach, Chen *et al.* (31) were able to identify 622 glycosylation sites from 5 mg of tryptic human liver protein digest, and when using two other enzymes, thermolysin and pepsin, in parallel experiments, they identified an additional 317 sites. In our ERLIC approach, enrichment and fractionation were achieved in a single step. The analysis of fractions by one-dimensional LC-MS/MS yielded 922 glycosylation sites and 544 glycoproteins from a relatively small amount of samples (3 mg). This represents 92.7% of the total identified glycosylation sites and 96.8% of the total glycoproteins. The hydrazide method provided an additional 73 glycosylation sites (7.3%) and 18 glycoproteins (3.2%). The higher percentage of new glycosylation sites over new glycoproteins from the hydrazide chemistry method suggests that higher glycosylation site coverage of each glycoprotein could be achieved when combining the ERLIC and hydrazide methods.

We next matched these 995 glycosylation sites with the newly released Swiss-Prot knowledge database for rodent

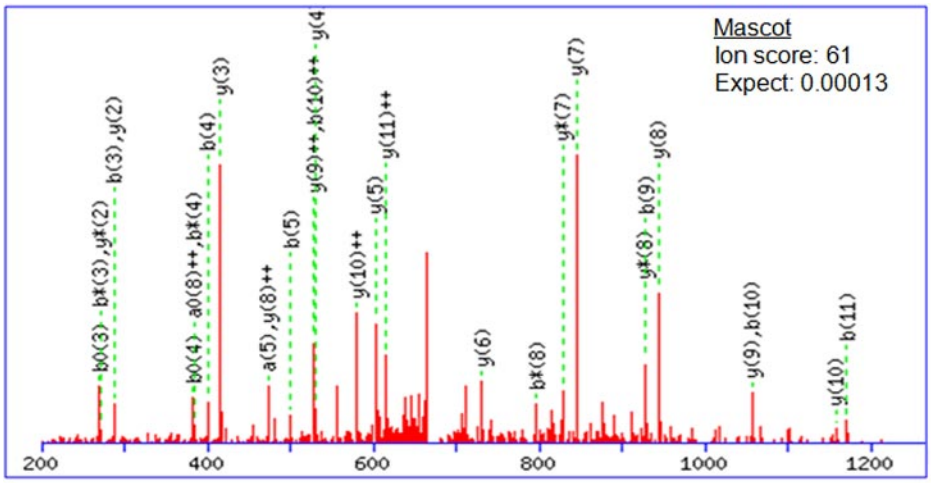

#	b	Seq.	y	y++	#
1	116.0342	N			12
2	187.0713	A	1229.685	615.3461	11
3	288.119	T	1158.648	579.8275	10
4	401.2031	L	1057.6	529.3037	9
5	500.2715	V	944.516	472.7616	8
6	614.3144	N	845.4476	423.2274	7
7	743.357	E	731.4046	366.206	6
8	814.3941	A	602.362	301.6847	5
9	929.4211	D	531.3249	266.1661	4
10	1057.516	K	416.298	208.6526	3
11	1170.6	L	288.203	144.6051	2
12		R	175.119	88.0631	1

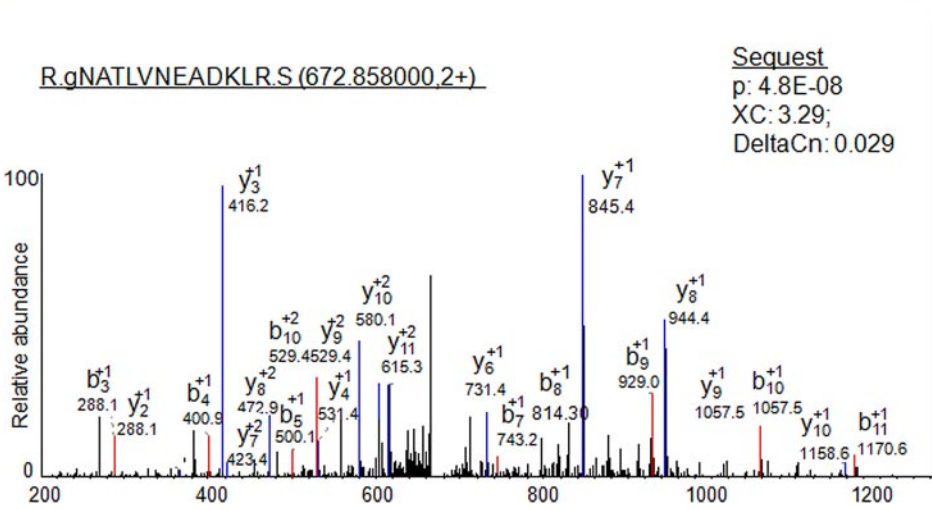

#	b	Seq.	y	y++	#
1	116.0342	N			12
2	187.0713	A	1229.685	615.3461	11
3	288.119	T	1158.648	579.8275	10
4	401.2031	L	1057.6	529.3037	9
5	500.2715	V	944.516	472.7616	8
6	614.3144	N	845.4476	423.2274	7
7	743.357	E	731.4046	366.206	6
8	814.3941	A	602.362	301.6847	5
9	929.4211	D	531.3249	266.1661	4
10	1057.516	K	416.298	208.6526	3
11	1170.6	L	288.203	144.6051	2
12		R	175.119	88.06311	1

FIG. 4. **Representative mass spectrum that was confidently assigned to peptide R ↓ gNATLVNEADKLR ↓ S from aminopeptidase N (CD13) by Mascot but not Sequest.**

species (released on May 26, 2009). It is worth mentioning that the positions of the glycosylation sites identified from the IPI database were different from those in the Swiss-Prot database in some of the glycoproteins. For example, CD98 heavy chain (IPI00114641) was identified with four glycosylation sites at Asn-172, Asn-265, Asn-391, and Asn-405, whereas in the Swiss-Prot database, these sites become Asn-166, Asn-259, Asn-385, and Asn-399 because of sequence cleavage or protein truncation/isoform. Such changes in site position were manually verified based on sequence match and included in supplemental Table 2. Of the 995 glycosylation sites, only 39 are documented as valid *N*-linked glycosylation sites with experimental proof of which two are high mannose type; 62.0% (617) of them are annotated as potential (601 sites), probable (five sites), or by similarity (11 sites); and 34.1% (339) of them were not documented as *N*-linked glycosylation sites (Fig. 6*a*). This shows that glycoproteins and glycosylation sites are largely underrepresented in the current databases, and the use of a glycoproteomics approach allows not only a large scale validation of potential glycosylation sites but also identification of novel glycosylation sites (Fig. 6*b*).

Identification of Membrane Phosphoproteins—Phosphorylation of membrane proteins often initiates signal transduction pathways or attenuates plasma membrane transport processes (54). However, study of these proteins is challenging due to the inherent hydrophobicity of membrane proteins and low abundance of phosphopeptides. Here, we prepared protein digests from purified membrane proteins and enriched hydrophilic and negatively charged peptides using ERLIC. We showed that in addition to the identification of a high number of glycoproteins a total of 383 phosphoproteins was also identified with 915 unique phosphorylation sites identified (supplemental Table 3). Of these, 232 proteins (60.1%) are membrane phosphoproteins, and 140 are known plasma membrane proteins, indicative of the efficacy of this approach for studying the membrane phosphoproteome. The MS/MS spectra of the ERLIC enriched phosphopeptides in Mascot peptide view format are shown in the supplemental Data 2 and 3. As shown in the MS/MS spectrum in the Mascot

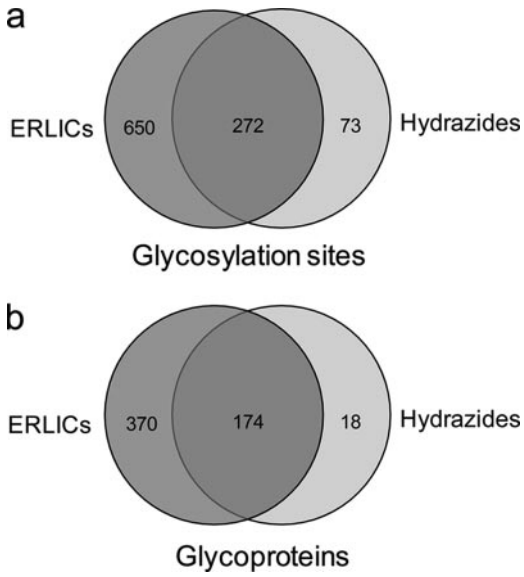

FIG. 5. **Venn diagrams of glycosylation sites (*a*) and glycoproteins (*b*) identified from ERLIC and the hydrazide method are shown.**

peptide view in the supplemental Data 3, the phosphorylation site of most phosphopeptides is sandwiched by fragments still bearing the modification as well as the corresponding neutral loss (−98 Da) fragments; *e.g.* in the phosphopeptide QADVPAAVTDAAATpTPAAEDAATK (where pT is phosphothreonine) shown in MS/MS Spectrum 1, the phosphorylation site is sandwiched with fragments y4, y5, y6, y7, y8, y12, y12 − 98, y14, and y14 − 98. The reliability of the phosphorylation site assignment can be determined by these fragments.

Notably, about 41.2% of these phosphoproteins were also identified as being glycosylated, demonstrating the potential of our protocol for simultaneous identification of both post-translational modifications in a single protein. For example, L1cam (neural cell adhesion molecule (NCAM) L1 precursor, IPI00115762) is predicted to have 21 potential N-linked glycosylation sites and six phosphorylation sites. Of these, we were able to identify 11 glycosylation and four phosphorylation sites. Glycosylation and phosphorylation may modulate protein function separately or in a cooperative way. For example, modulation of L1 function by NCAM occurs through the recognition of L1 carbohydrate, whereas phosphorylation of its tyrosine and serine regulates cytoplasmic interactions, L1 mobility, and internalization (55). Simultaneous monitoring of the two types of modifications might provide more insights into the functions of the protein of interest.

Distribution of Glyco- and Phosphopeptides in ERLIC—Fig. 7*a* shows that the average number of peptides identified from each fraction decreased slightly from fraction 1 to 7, but the ratio of glyco- and phosphopeptides over other peptides changed from about 20 to 80% (Fig. 7*b*), confirming that these two modified peptides had an elution profile different from that of other peptides under our two-buffer elution system. In addition, we observed that phosphopeptides were eluted earlier with more peptides in the earlier fractions and fewer in the later fractions. In contrast, glycopeptides eluted later with fewer glycopeptides in the earlier fractions and more in the later fractions. This suggests that the use of ERLIC could not only simultaneously enrich glyco- and phosphopeptides but also differentially fractionate peptides into glycopeptides and phosphopeptides by using an optimized elution gradient.

Functional Annotation of Identified Glycoproteins—Of the 562 identified glycoproteins, 329 proteins have a predicted signal sequence, and 405 proteins were predicted to contain transmembrane domains. Most of them contained either one or two transmembrane domains, but as many as 198 proteins with ≥3 transmembrane domains were also identified. Based on these data, 91.1% of the proteins were further classified as extracellular proteins consisting of cell surface, secreted, and transmembrane proteins. This is consistent with the subcellular classification of these proteins using GO from MGI. As shown in Fig. 8*a*, the higher abundance groups consist of plasma membrane/other membrane (71%), endoplasmic reticulum/Golgi (9%), and extracellular matrix proteins (9%), whereas intracellular proteins only account for 11% of total identified glycoproteins of which less than 1% are of cytosolic origin. The assignment of *N*-glycoproteins, at least some of them, to intracellular origin might be due to GO annotation error or the presence of the extracellular form of the protein (14). Thus, enrichment of glycopeptides is not only essential to the study of protein glycosylation but is also an effective approach to identify membrane proteins, which are underrepresented in the database because of their hydrophobicity.

Glycoproteins in the brain are involved in various processes such as cell migration, neurite outgrowth and fasciculation, synapse formation and stabilization, and modulation of synaptic efficacy (56). As expected, the majority of the identified proteins were involved in transport (17%), development process (15%), signal transduction (12%), or cell adhesion (12%) (Fig. 8*b*). Only a modest number of proteins were associated with processes involved in the rare events of neural regeneration such as cell death (4%), cell cycle and proliferation (3%), and RNA metabolism (1%). As shown in Fig. 8*c*, the major molecular functions of the identified glycoproteins were binding activity (29%), catalytic activity (19%), and transporter activity (17%). Further pathway analysis of identified glycoproteins by KEGG mapped eight significant pathways ($p < 0.05$) (Fig. 8*d*). As neurons constitute a core component of the brain, as expected, most of the identified proteins were from pathways directly involved in neuron activity such as neuroactive ligand-receptor interaction, calcium signaling, axon guidance, and long term potentiation.

Identification of Disease-related Glycoproteins—Glycoproteins and their attached glycans have pivotal roles in nervous system development, regeneration, and synaptic plasticity. Alteration of *N*-glycans in humans results in many congenital and chronic neurological disorders such as epilepsy, ataxia,

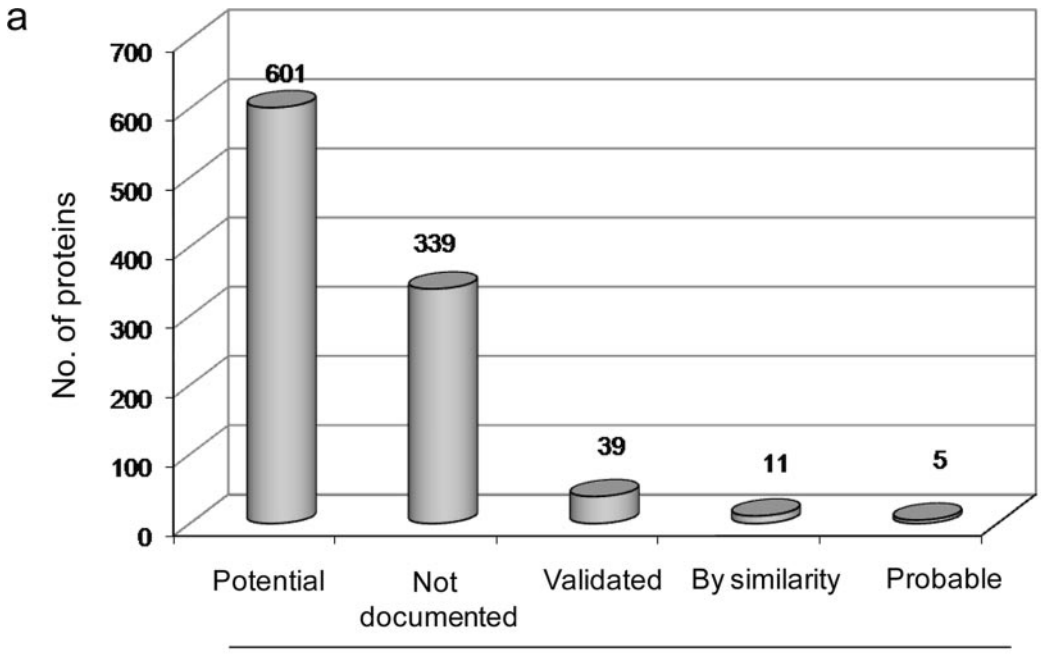

b

R.GETASLLCgNISVR.G (710.8569,2+), ion score 83, expect 1.2e-06

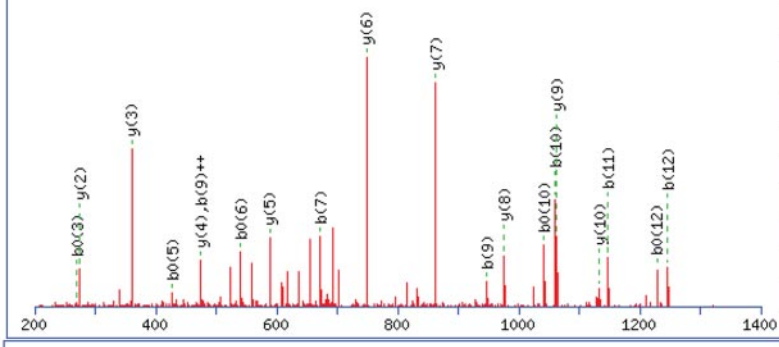

#	b	Seq.	y	#
1	58.0287	G		13
2	187.0713	E	1363.689	12
3	288.119	T	1234.646	11
4	359.1561	A	1133.598	10
5	446.1882	S	1062.561	9
6	559.2722	L	975.5292	8
7	672.3563	L	862.4451	7
8	832.3869	C	749.361	6
9	947.4139	N	589.3304	5
10	1060.498	I	474.3035	4
11	1147.53	S	361.2194	3
12	1246.598	V	274.1874	2
13		R	175.119	1

c

K.DYGgNYTCVATNK.L (703.796500,2+) , ion score 73, expect 1.2e-05

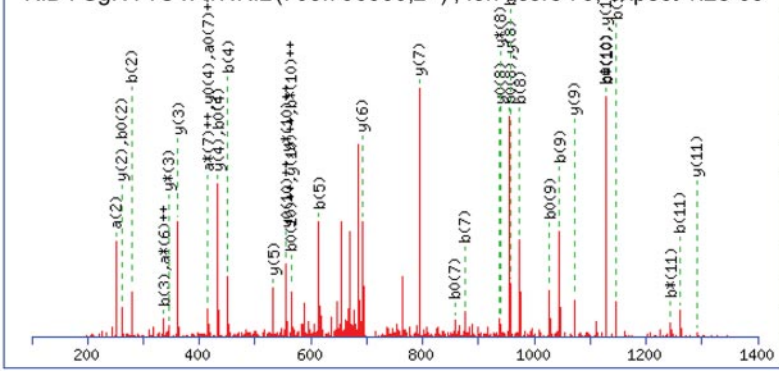

#	b	Seq.	y	#
1	116.0342	D		12
2	279.0975	Y	1291.562	11
3	336.119	G	1128.499	10
4	451.1459	N	1071.478	9
5	614.2093	Y	956.4506	8
6	715.257	T	793.3873	7
7	875.2876	C	692.3396	6
8	974.356	V	532.3089	5
9	1045.393	A	433.2405	4
10	1146.441	T	362.2034	3
11	1260.484	N	261.1557	2
12		K	147.1128	1

FIG. 6. **Annotation of identified glycosylation sites.** *a*, matches of identified glycosylation sites with the Swiss-Prot knowledge database of rodent. *b*, spectrum for identification of a novel glycosylation site in R ↓ GETASLLCgNISVR ↓ G (*m/z* = 710.857, *z* = 2+) in Igsf8 (immunoglobulin superfamily member 8 precursor, IPI00321348). Igsf8 has three potential sites; we found all of them as well as a novel site, Asn-461 (shown). *c*, spectrum for identification of a glycosylation site in K ↓ DYGgNYTCVATNK ↓ L (*m/z* = 703.797, *z* = 2+) in Opcml (opioid-binding cell adhesion molecule, IPI00463489). This protein was not documented in the Swiss-Prot database.

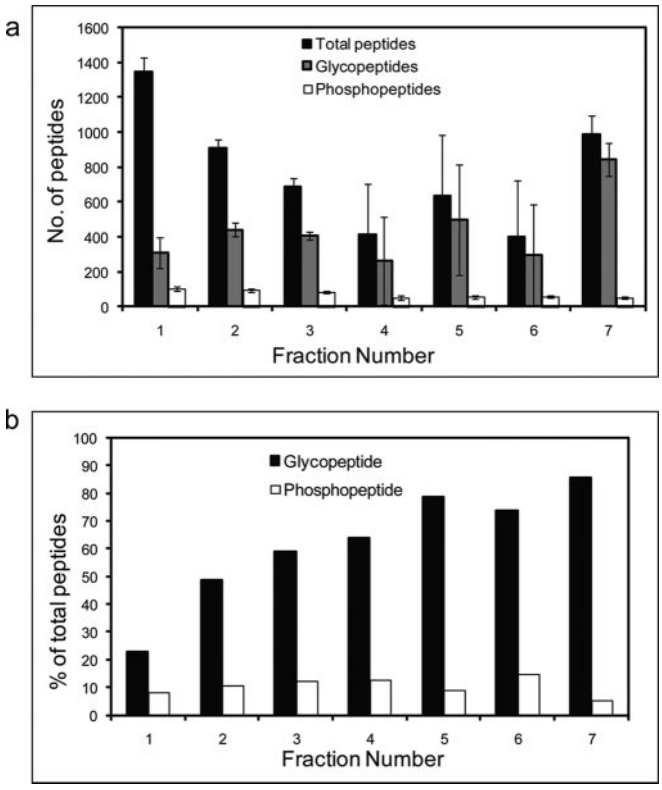

FIG. 7. **Distribution of peptides in seven fractions collected from ERLIC.** Peptides used are above peptide identity cutoff scores of the Mascot database search. *a*, average number of peptides, glycopeptides, and phosphopeptides identified in each fraction from six replicates. *Error bars* are the S.D. *b*, percentage of glyco- and phosphopeptides identified in each fraction.

cerebellar and cerebral atrophy, and abnormal eye movements (56). The severity of these diseases is largely dependent on the extent of the *N*-glycan impairment.

The mouse brain glycoproteins have an *N*-glycan profile similar to that of glycoproteins from human (57), which suggests that information derived from the study of mouse brain could be of significance in human. In this study, we found a number of glycoproteins that are known to be related to various neurological disorders (supplemental Table 4). The major prion protein (Prnp) has two potential *N*-glycosylation sites, mutations in which have been associated with aging and prion disease such as Creutzfeldt-Jakob disease (58, 59). The tripeptidyl-peptidase 1 (TPP1) has a role in regulation of intracellular lipopigment storage material. A defect in the *N*-glycosylation of Asp-286 results in accumulation of those materials and is clinically characterized with neuronal ceroid lipofuscinoses (60, 61). In Alzheimer disease, the clinical feature is the formation of extracellular amyloid plaque in the brain, which is putatively caused by a mutation in the amyloid β precursor protein (APP) and/or its regulators (62). Recently, alteration of the glycosylation of APP was implicated in Alzheimer disease (63). Here, we identified not only APP but also its regulators such as membrane metalloendopeptidase (Mme) and protein phosphatase 3, catalytic subunit, α isoform (Ppp3ca). Mme has a role in the degradation of excess and misfolded APP peptide (64), and the activity of protein phosphatase tightly regulates APP secretion (65). In addition, we found six proteins that are related to diabetes, a disease characterized by insulin resistance and hyperinsulinemia. Insulin signaling has an important role in neuronal growth and differentiation (66), and a decrease in the number or defects in the function of insulin receptors in the brain has been implicated in the development of type 2 diabetes (67). As a result, type 2 diabetes has been proposed as a brain disorder (68). The identification of abundant diabetes-related proteins in the mouse brain might provide support of this classification.

Many other disease-related proteins such as Niemann-Pick C1 protein (NPC1) (Niemann-Pick type C disease), solute carrier family 18, member 2 (Slc18a2) (Parkinson disease), and L1 cell adhesion molecule (MASA (mental retardation, aphasia, shuffling gait, and adducted thumbs) syndrome) were also identified. Most of these diseases are caused not only by abnormal protein expression but also by aberrant glycosylation. Importantly, in the ERLIC approach, the glycopeptide and its glycan are recovered together, permitting a further detailed glycan analysis. This is in contrast to the hydrazide chemistry method where glycan information is lost during the recovery of glycopeptides.

Conclusion—The geriatric proportion of the population is growing faster worldwide, and it has been estimated that by the year 2020 over 70% of the global burden of diseases in developing and newly industrialized countries will be contributed by degenerative illness apart from cardiovascular diseases, cancer, and others (69). Aberrant glycosylation and phosphorylation have been implicated in numerous acute and chronic neurological disorders (7–9) for which effective noninvasive diagnostic tools or successful therapies have yet to become available. Hence, understanding the molecular mechanism at the level of proteins and their post-translational modifications could facilitate the identification of therapeutic targets or potential biomarkers for these disorders. Here, we studied the mouse brain glycoproteome using an optimized ERLIC as well as the hydrazide chemistry approach. We report a total of 562 glycoproteins and 995 glycosylation sites, representing the largest data set of brain-derived glycoproteome documented so far. About 96% of the identified glycosylation sites are new as they are either not recorded or annotated as putative glycosylation sites in the curated Swiss-Prot database. Of the 562 glycoproteins, 13.7% (77) of them are known to be related to various neurological disorders, providing a potential value to understand the mechanism of brain disease and to identify novel disease biomarkers.

We showed here that the ERLIC approach is more efficient in the identification of glycopeptides and glycoproteins than the hydrazide chemistry method (Fig. 5). A bonus is that ERLIC enriches glycopeptides without destroying their attached glycan, which could permit further glycan analysis.

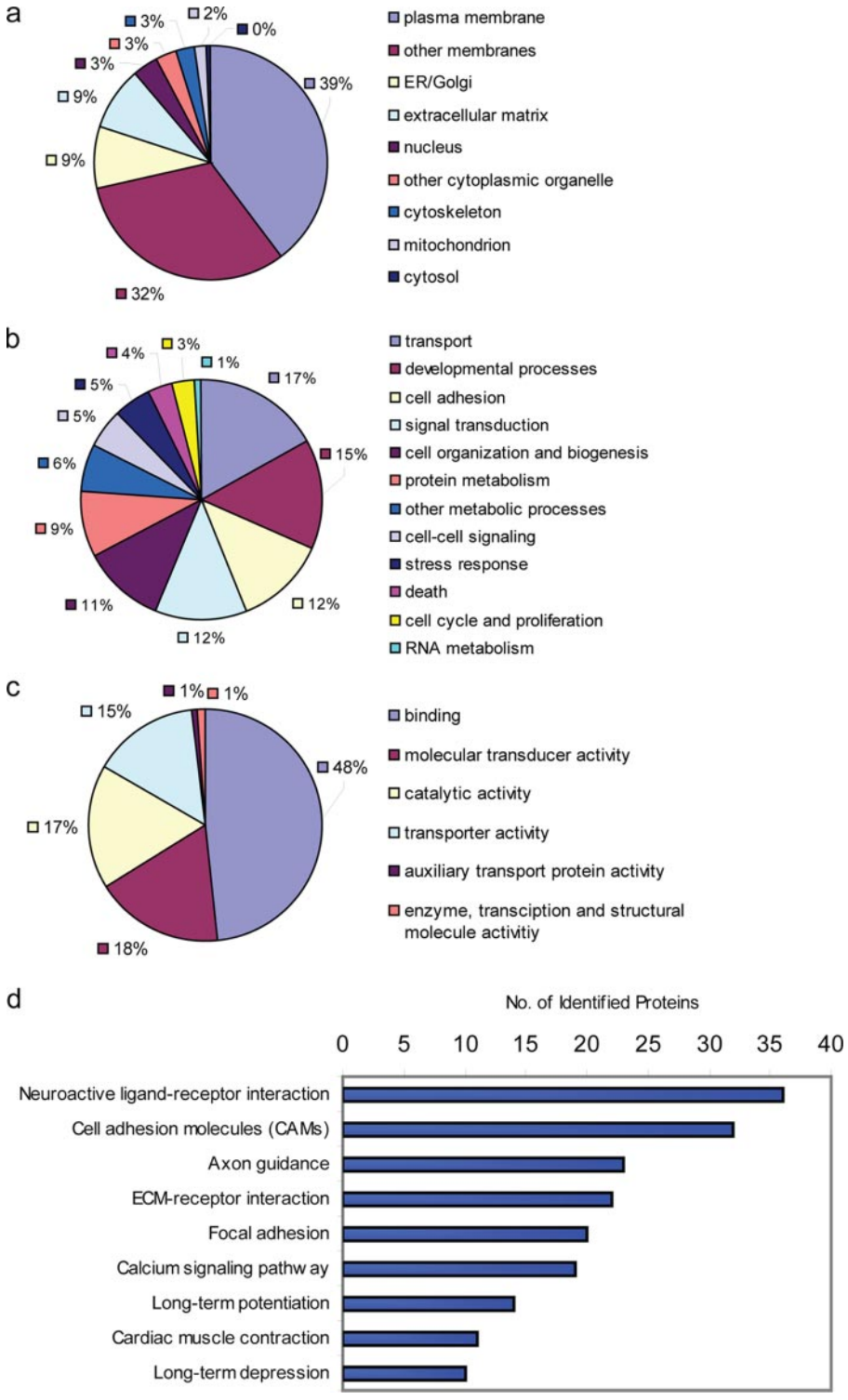

FIG. 8. **Functional analysis of identified glycoproteins.** Gene ontology classification of identified glycoproteins is shown: subcellular location (*a*), biological process (*b*), and molecular function group (*c*) using MGI GO_Slim Chart Tool and KEGG pathway analysis (*d*). *ER*, endoplasmic reticulum; *ECM*, extracellular matrix.

Additionally, ERLIC, which has been shown to be efficient in enriching for phosphopeptides (42, 43), can be adapted to simultaneously enrich for both glycopeptides and phosphopeptides that together represent proteins with the two most important post-translational modifications. Some of the identified proteins had both glycosylation and phosphorylation modifications. For example, we identified 11 glycosylation sites and four phosphorylation sites in NCAM L1 precursor. Simultaneous identification of two types of post-translational modifications is not only useful for studying the function of a single protein but also helps to elucidate systemic changes of the whole proteome at different cell states.

In summary, we demonstrate that ERLIC is a simple and robust approach for not only the recovery of glycoproteins but also the simultaneous recovery of both glycoproteins and phosphoproteins. This approach enabled us to identify the largest set of glycoproteins from mouse brain so far, which could be of significant value in complementing the current glycoprotein database. We expect that ERLIC could help to uncover more glycoproteins and novel glycosylation sites from other samples such as body fluid, cells, or tissues.

Supplemental Data—Detailed information on all identified proteins is listed in supplemental Table 5 (from the Mascot search) and supplemental Table 6 (from the Sequest search). All MS^2 spectra of glyco- and phosphopeptide assignments are clearly shown in supplemental spectra hosted on https://proteomecommons.org/tranche/ (titled "Simultaneous Characterization of Glyco- and Phospho-proteomes of Mouse Brain Membrane Proteome Using ERLIC Chromatography") and downloadable using the following hash: LCcjHCB0H/g-7PpRF7Q5uAo0vh2MIEWGi56q8jy/dqQ3OBOk6JNsXXU-PoyUEgctUS+BmB1PpyRSOYRc54Mu46im1RxeoAAAAAA-AACwA==. Alternatively, the non-redundant MS^2 spectra of glyco- and phosphopeptide assignments are provided in Supplemental Data 1–4.

Acknowledgment—We express our gratitude to Andrew Alpert of PolyLC, Inc. for invaluable advice. We thank Wei Meng, Yi Zhu, Paul Hon Sen Tan, and Manavalan Arulmani for invaluable discussions.

* This work was supported by Biomedical Research Council Grant 07/1/22/19/531 and Ministry of Education ARC Grant T206B3211 of Singapore.

S This article contains supplemental Tables 1–6 and spectral Data 1–4.

¶ To whom correspondence should be addressed. Tel.: 65-6514-1006; Fax: 65-6791-3856; E-mail: sksze@ntu.edu.sg.

REFERENCES

1. Apweiler, R., Hermjakob, H., and Sharon, N. (1999) On the frequency of protein glycosylation, as deduced from analysis of the SWISS-PROT database. *Biochim. Biophys. Acta* **1473,** 4–8
2. Cohen, P. (2000) The regulation of protein function by multisite phosphorylation–a 25 year update. *Trends Biochem. Sci.* **25,** 596–601
3. Roth, J. (2002) Protein N-glycosylation along the secretory pathway: relationship to organelle topography and function, protein quality control, and cell interactions. *Chem. Rev.* **102,** 285–303
4. Schmidt-Ullrich, R. K., Contessa, J. N., Lammering, G., Amorino, G., and Lin, P. S. (2003) ERBB receptor tyrosine kinases and cellular radiation responses. *Oncogene* **22,** 5855–5865
5. Dennis, J. W., Granovsky, M., and Warren, C. E. (1999) Protein glycosylation in development and disease. *BioEssays* **21,** 412–421
6. Ballif, B. A., Villén, J., Beausoleil, S. A., Schwartz, D., and Gygi, S. P. (2004) Phosphoproteomic analysis of the developing mouse brain. *Mol. Cell. Proteomics* **3,** 1093–1101
7. Guevara, J., Espinosa, B., Zenteno, E., Vázguez, L., Luna, J., Perry, G., and Mena, R. (1998) Altered glycosylation pattern of proteins in Alzheimer disease. *J. Neuropathol. Exp. Neurol.* **57,** 905–914
8. Takahashi, M., Tsujioka, Y., Yamada, T., Tsuboi, Y., Okada, H., Yamamoto, T., and Liposits, Z. (1999) Glycosylation of microtubule-associated protein tau in Alzheimer's disease brain. *Acta Neuropathol.* **97,** 635–641
9. Mi, K., and Johnson, G. V. (2006) The role of tau phosphorylation in the pathogenesis of Alzheimer's disease. *Curr. Alzheimer Res.* **3,** 449–463
10. Castellani, R., Smith, M. A., Richey, P. L., and Perry, G. (1996) Glycoxidation and oxidative stress in Parkinson disease and diffuse Lewy body disease. *Brain Res.* **737,** 195–200
11. Muntané, G., Dalfó, E., Martinez, A., and Ferrer, I. (2008) Phosphorylation of tau and alpha-synuclein in synaptic-enriched fractions of the frontal cortex in Alzheimer's disease, and in Parkinson's disease and related alpha-synucleinopathies. *Neuroscience* **152,** 913–923
12. Guerry, P. (1997) Nonlipopolysaccharide surface antigens of Campylobacter species. *J. Infect. Dis.* **176,** Suppl. 2, S122–S124
13. Liu, J., Ball, S. L., Yang, Y., Mei, P., Zhang, L., Shi, H., Kaminski, H. J., Lemmon, V. P., and Hu, H. (2006) A genetic model for muscle-eye-brain disease in mice lacking protein O-mannose 1,2-N-acetylglucosaminyltransferase (POMGnT1). *Mech. Dev.* **123,** 228–240
14. Zhang, H., Loriaux, P., Eng, J., Campbell, D., Keller, A., Moss, P., Bonneau, R., Zhang, N., Zhou, Y., Wollscheid, B., Cooke, K., Yi, E. C., Lee, H., Peskind, E. R., Zhang, J., Smith, R. D., and Aebersold, R. (2006) UniPep—a database for human N-linked glycosites: a resource for biomarker discovery. *Genome Biol.* **7,** R73
15. Chalmers, M. J., Kolch, W., Emmett, M. R., Marshall, A. G., and Mischak, H. (2004) Identification and analysis of phosphopeptides. *J. Chromatogr. B Analyt. Technol. Biomed. Life Sci.* **803,** 111–120
16. Mintz, G., and Glaser, L. (1979) Glycoprotein purification on a high-capacity wheat germ lectin affinity column. *Anal. Biochem.* **97,** 423–427
17. Mechref, Y., Madera, M., and Novotny, M. V. (2008) Glycoprotein enrichment through lectin affinity techniques. *Methods Mol. Biol.* **424,** 373–396
18. Drake, R. R., Schwegler, E. E., Malik, G., Diaz, J., Block, T., Mehta, A., and Semmes, O. J. (2006) Lectin capture strategies combined with mass spectrometry for the discovery of serum glycoprotein biomarkers. *Mol. Cell. Proteomics* **5,** 1957–1967
19. Hourani, B. T., Chace, N. M., and Pincus, J. H. (1973) Plasma membrane glycoproteins from nucleated cells. I. Preparative techniques for isolation and partial characterization of a membrane glycoprotein extract from L1210 cells with lectin receptor activity. *Biochim. Biophys. Acta* **328,** 520–532
20. Debray, H., Decout, D., Strecker, G., Spik, G., and Montreuil, J. (1981) Specificity of twelve lectins towards oligosaccharides and glycopeptides related to N-glycosylproteins. *Eur. J. Biochem.* **117,** 41–55
21. Ghosh, D., Krokhin, O., Antonovici, M., Ens, W., Standing, K. G., Beavis, R. C., and Wilkins, J. A. (2004) Lectin affinity as an approach to the proteomic analysis of membrane glycoproteins. *J. Proteome Res.* **3,** 841–850
22. Lee, A., Kolarich, D., Haynes, P. A., Jensen, P. H., Baker, M. S., and Packer, N. H. (2009) Rat liver membrane glycoproteome: enrichment by phase partitioning and glycoprotein capture. *J. Proteome Res.* **8,** 770–781
23. Wada, Y., Tajiri, M., and Yoshida, S. (2004) Hydrophilic affinity isolation and MALDI multiple-stage tandem mass spectrometry of glycopeptides for glycoproteomics. *Anal. Chem.* **76,** 6560–6565
24. Tajiri, M., Yoshida, S., and Wada, Y. (2005) Differential analysis of site-specific glycans on plasma and cellular fibronectins: application of a hydrophilic affinity method for glycopeptide enrichment. *Glycobiology* **15,** 1332–1340
25. Ding, W., Nothaft, H., Szymanski, C. M., and Kelly, J. (2009) Identification and quantification of glycoproteins using ion-pairing normal-phase liquid chromatography and mass spectrometry. *Mol. Cell. Proteomics* **8,** 2170–2185
26. Zhang, H., Li, X. J., Martin, D. B., and Aebersold, R. (2003) Identification and quantification of N-linked glycoproteins using hydrazide chemistry, stable isotope labeling and mass spectrometry. *Nat. Biotechnol.* **21,** 660–666
27. Sun, B., Ranish, J. A., Utleg, A. G., White, J. T., Yan, X., Lin, B., and Hood, L. (2007) Shotgun glycopeptide capture approach coupled with mass spectrometry for comprehensive glycoproteomics. *Mol. Cell. Proteomics* **6,** 141–149
28. Zhang, H., Yi, E. C., Li, X. J., Mallick, P., Kelly-Spratt, K. S., Masselon, C. D., Camp, D. G., 2nd, Smith, R. D., Kemp, C. J., and Aebersold, R. (2005) High throughput quantitative analysis of serum proteins using glycopeptide capture and liquid chromatography mass spectrometry. *Mol. Cell. Proteomics* **4,** 144–155
29. Ramachandran, P., Boontheung, P., Xie, Y., Sondej, M., Wong, D. T., and Loo, J. A. (2006) Identification of N-linked glycoproteins in human saliva by glycoprotein capture and mass spectrometry. *J. Proteome Res.* **5,** 1493–1503

30. Lewandrowski, U., Moebius, J., Walter, U., and Sickmann, A. (2006) Elucidation of N-glycosylation sites on human platelet proteins: a glycoproteomic approach. *Mol. Cell. Proteomics* **5,** 226–233
31. Chen, R., Jiang, X., Sun, D., Han, G., Wang, F., Ye, M., Wang, L., and Zou, H. (2009) Glycoproteomics analysis of human liver tissue by combination of multiple enzyme digestion and hydrazide chemistry. *J. Proteome Res.* **8,** 651–661
32. Zhang, H., Liu, A. Y., Loriaux, P., Wollscheid, B., Zhou, Y., Watts, J. D., and Aebersold, R. (2007) Mass spectrometric detection of tissue proteins in plasma. *Mol. Cell. Proteomics* **6,** 64–71
33. Cao, J., Shen, C., Wang, H., Shen, H., Chen, Y., Nie, A., Yan, G., Lu, H., Liu, Y., and Yang, P. (2009) Identification of N-glycosylation sites on secreted proteins of human hepatocellular carcinoma cells with a complementary proteomics approach. *J. Proteome Res.* **8,** 662–672
34. Tao, W. A., Wollscheid, B., O'Brien, R., Eng, J. K., Li, X. J., Bodenmiller, B., Watts, J. D., Hood, L., and Aebersold, R. (2005) Quantitative phosphoproteome analysis using a dendrimer conjugation chemistry and tandem mass spectrometry. *Nat. Methods* **2,** 591–598
35. Rush, J., Moritz, A., Lee, K. A., Guo, A., Goss, V. L., Spek, E. J., Zhang, H., Zha, X. M., Polakiewicz, R. D., and Comb, M. J. (2005) Immunoaffinity profiling of tyrosine phosphorylation in cancer cells. *Nat. Biotechnol.* **23,** 94–101
36. Ficarro, S. B., McCleland, M. L., Stukenberg, P. T., Burke, D. J., Ross, M. M., Shabanowitz, J., Hunt, D. F., and White, F. M. (2002) Phosphoproteome analysis by mass spectrometry and its application to Saccharomyces cerevisiae. *Nat. Biotechnol.* **20,** 301–305
37. Beausoleil, S. A., Jedrychowski, M., Schwartz, D., Elias, J. E., Villén, J., Li, J., Cohn, M. A., Cantley, L. C., and Gygi, S. P. (2004) Large-scale characterization of HeLa cell nuclear phosphoproteins. *Proc. Natl. Acad. Sci. U.S.A.* **101,** 12130–12135
38. Larsen, M. R., Thingholm, T. E., Jensen, O. N., Roepstorff, P., and Jørgensen, T. J. (2005) Highly selective enrichment of phosphorylated peptides from peptide mixtures using titanium dioxide microcolumns. *Mol. Cell. Proteomics* **4,** 873–886
39. Villén, J., Beausoleil, S. A., Gerber, S. A., and Gygi, S. P. (2007) Large-scale phosphorylation analysis of mouse liver. *Proc. Natl. Acad. Sci. U.S.A.* **104,** 1488–1493
40. Olsen, J. V., Blagoev, B., Gnad, F., Macek, B., Kumar, C., Mortensen, P., and Mann, M. (2006) Global, in vivo, and site-specific phosphorylation dynamics in signaling networks. *Cell* **127,** 635–648
41. Bodenmiller, B., Mueller, L. N., Mueller, M., Domon, B., and Aebersold, R. (2007) Reproducible isolation of distinct, overlapping segments of the phosphoproteome. *Nat. Methods* **4,** 231–237
42. Alpert, A. J. (2008) Electrostatic repulsion hydrophilic interaction chromatography for isocratic separation of charged solutes and selective isolation of phosphopeptides. *Anal. Chem.* **80,** 62–76
43. Gan, C. S., Guo, T., Zhang, H., Lim, S. K., and Sze, S. K. (2008) A comparative study of electrostatic repulsion-hydrophilic interaction chromatography (ERLIC) versus SCX-IMAC-based methods for phosphopeptide isolation/enrichment. *J. Proteome Res.* **7,** 4869–4877
44. Lewandrowski, U., Lohrig, K., Zahedi, R., Walter, D., and Sickmann, A. (2008) Glycosylation site analysis of human platelets by electrostatic repulsion hydrophilic interaction chromatography. *Clin. Proteomics* **4,** 25–36
45. Kersey, P. J., Duarte, J., Williams, A., Karavidopoulou, Y., Birney, E., and Apweiler, R. (2004) The International Protein Index: an integrated database for proteomics experiments. *Proteomics* **4,** 1985–1988
46. Guo, T., Gan, C. S., Zhang, H., Zhu, Y., Kon, O. L., and Sze, S. K. (2008) Hybridization of pulsed-Q dissociation and collision-activated dissociation in linear ion trap mass spectrometer for iTRAQ quantitation. *J. Proteome Res.* **7,** 4831–4840
47. Elias, J. E., and Gygi, S. P. (2007) Target-decoy search strategy for increased confidence in large-scale protein identifications by mass spectrometry. *Nat. Methods* **4,** 207–214
48. Bendtsen, J. D., Nielsen, H., von Heijne, G., and Brunak, S. (2004) Improved prediction of signal peptides: SignalP 3.0. *J. Mol. Biol.* **340,** 783–795
49. Krogh, A., Larsson, B., von Heijne, G., and Sonnhammer, E. L. (2001) Predicting transmembrane protein topology with a hidden Markov model: application to complete genomes. *J. Mol. Biol.* **305,** 567–580
50. Mi, H., Lazareva-Ulitsky, B., Loo, R., Kejariwal, A., Vandergriff, J., Rabkin, S., Guo, N., Muruganujan, A., Doremieux, O., Campbell, M. J., Kitano, H., and Thomas, P. D. (2005) The PANTHER database of protein families, subfamilies, functions and pathways. *Nucleic Acids Res.* **33,** D284–D288
51. Zhang, H., Lin, Q., Ponnusamy, S., Kothandaraman, N., Lim, T. K., Zhao, C., Kit, H. S., Arijit, B., Rauff, M., Hew, C. L., Chung, M. C., Joshi, S. B., and Choolani, M. (2007) Differential recovery of membrane proteins after extraction by aqueous methanol and trifluoroethanol. *Proteomics* **7,** 1654–1663
52. Danziger, R. S. (2008) Aminopeptidase N in arterial hypertension. *Heart Fail. Rev.* **13,** 293–298
53. Elias, J. E., Haas, W., Faherty, B. K., and Gygi, S. P. (2005) Comparative evaluation of mass spectrometry platforms used in large-scale proteomics investigations. *Nat. Methods* **2,** 667–675
54. Thingholm, T. E., Larsen, M. R., Ingrell, C. R., Kassem, M., and Jensen, O. N. (2008) TiO(2)-based phosphoproteomic analysis of the plasma membrane and the effects of phosphatase inhibitor treatment. *J. Proteome Res.* **7,** 3304–3313
55. Kenwrick, S., Watkins, A., and De Angelis, E. (2000) Neural cell recognition molecule L1: relating biological complexity to human disease mutations. *Hum. Mol. Genet.* **9,** 879–886
56. Kleene, R., and Schachner, M. (2004) Glycans and neural cell interactions. *Nat. Rev. Neurosci.* **5,** 195–208
57. Albach, C., Klein, R. A., and Schmitz, B. (2001) Do rodent and human brains have different N-glycosylation patterns? *Biol. Chem.* **382,** 187–194
58. Owen, F., Poulter, M., Lofthouse, R., Collinge, J., Crow, T. J., Risby, D., Baker, H. F., Ridley, R. M., Hsiao, K., and Prusiner, S. B. (1989) Insertion in prion protein gene in familial Creutzfeldt-Jakob disease. *Lancet* **1,** 51–52
59. Goh, A. X., Li, C., Sy, M. S., and Wong, B. S. (2007) Altered prion protein glycosylation in the aging mouse brain. *J. Neurochem.* **100,** 841–854
60. Mole, S. E. (2006) Neuronal ceroid lipofuscinoses (NCL). *Eur. J. Paediatr. Neurol.* **10,** 255–257
61. Tsiakas, K., Steinfeld, R., Storch, S., Ezaki, J., Lukacs, Z., Kominami, E., Kohlschütter, A., Ullrich, K., and Braulke, T. (2004) Mutation of the glycosylated asparagine residue 286 in human CLN2 protein results in loss of enzymatic activity. *Glycobiology* **14,** 1C–5C
62. Sennvik, K., Fastbom, J., Blomberg, M., Wahlund, L. O., Winblad, B., and Benedikz, E. (2000) Levels of alpha- and beta-secretase cleaved amyloid precursor protein in the cerebrospinal fluid of Alzheimer's disease patients. *Neurosci. Lett.* **278,** 169–172
63. Akasaka-Manya, K., Manya, H., Sakurai, Y., Wojczyk, B. S., Spitalnik, S. L., and Endo, T. (2008) Increased bisecting and core-fucosylated N-glycans on mutant human amyloid precursor proteins. *Glycoconj. J.* **25,** 775–786
64. Helisalmi, S., Hiltunen, M., Vepsäläinen, S., Iivonen, S., Mannermaa, A., Lehtovirta, M., Koivisto, A. M., Alafuzoff, I., and Soininen, H. (2004) Polymorphisms in neprilysin gene affect the risk of Alzheimer's disease in Finnish patients. *J. Neurol. Neurosurg. Psychiatry* **75,** 1746–1748
65. Tian, Q., and Wang, J. (2002) Role of serine/threonine protein phosphatase in Alzheimer's disease. *Neurosignals* **11,** 262–269
66. Wan, Q., Xiong, Z. G., Man, H. Y., Ackerley, C. A., Braunton, J., Lu, W. Y., Becker, L. E., MacDonald, J. F., and Wang, Y. T. (1997) Recruitment of functional GABA(A) receptors to postsynaptic domains by insulin. *Nature* **388,** 686–690
67. Brüning, J. C., Gautam, D., Burks, D. J., Gillette, J., Schubert, M., Orban, P. C., Klein, R., Krone, W., Müller-Wieland, D., and Kahn, C. R. (2000) Role of brain insulin receptor in control of body weight and reproduction. *Science* **289,** 2122–2125
68. Das, U. N. (2002) Is type 2 diabetes mellitus a disorder of the brain? *Nutrition* **18,** 667–672
69. World Health Organization (2002) *Active Ageing: a Policy Framework*, World Health Organization, Geneva